Spillway stilling Basin Linings Design using Physical Hydraulic Modelling and DES CFD Modelling: Application of New Technologies

[1]Shayan Maleki, [2]James Willey [3]James Apostolidis, and [4]Virgilio Fiorotto

[1]*Ph.D, Technical Director – Dams, GHD Pty Ltd*

[2]*Senior Technical Director – Dams, GHD Pty Ltd*

[3]*CFD Modelling Specialist, GHD Pty Ltd*

[4]*Full Professor, University of Trieste*

The evaluation of the maximum instantaneous uplift force produced by turbulent pressure fluctuations plays a key role in designing concrete slab protection in spillway chutes and stilling basins. Recent incidents involving damage to chute linings have highlighted the significance of this issue.

To evaluate the stability of spillway stilling basin slabs, it is necessary to determine the statistical structure of the turbulent pressure fluctuations in the spillway chute and stilling basin. This can be defined by an extensive experimental work with a scale Physical Hydraulic Model (PHM). This exercise can be prohibitively expensive in terms of time and cost and it is proposed that the use of Computational Fluid Dynamics (CFD) in this application could become a cost effective alternative. A new approach using Detached Eddy Simulation (DES) was applied to the case of a scale physical hydraulic model representing a real-world prototype and the results of the simulation were compared with the direct laboratory measurements. Here the forces and pressures acting on the slabs are evaluated using both CFD and physical hydraulic modelling results.

In conclusion, some considerations on the design of slabs with unsealed joints are reported and discussed.

Keywords: *Spillway; Stilling basin; Lining; Dam; Physical hydraulic model; Computational fluid dynamics*

Introduction

A hydraulic jump is a rapidly varied phenomenon in free surface flow. It corresponds to a discontinuous transition from supercritical to subcritical flows in an open channel. A hydraulic jump includes several features by which excess mechanical energy may be dissipated through friction and conversion to heat. Hydraulic jumps downstream of high dams are often used as a solution for dissipation of water energy from floods.

The stability of concrete slab protection downstream of the dams or at the base of plunge pools downstream of large dams came to prominence when the slab protection in hydraulic jump stilling basins in some hydraulic plants was seriously damaged by floods smaller than maximum design event. Most notable cases include Malpaso, Tarbela and Karnafuli dams. In the former case, the 100 m head stilling basins underwent complete dislodgment of several slabs, each weighing approximately 730,000 kg. The spillway discharge causing the damage peaked at one-third of the design flood tested in a 1:100 model (Sànchez Bribiesca and Capella Viscaìno 1973). In the latter case (e.g. Bowers & Toso 1988), a discharge of about 20% the design discharge of 18,000 m³/s produced extensive damage to the chute floor over an area about 180 m wide and 23 m long. Questions have therefore been raised on whether conventional design criteria (e.g. Design of small dams 1987), based on steady seepage uplift, are adequate for high-head dissipation structures.

Numerous studies (e.g., Sanchez Bribiesca and Capella Viscaino 1973; Bowers and Tsai 1969; Bowers and Toso 1988) all agreed that the displacement of large concrete slabs were due to the intense, large, low frequency turbulent pressure fluctuations. It was pointed out that the reduction in the stability of the slabs is due to the severe pulsating pressures on the slab, in particular it was noted that:

- The pressure fluctuations may damage the sealed joints of the slabs and, through the unsealed joints, extreme pressure values may propagate from the upper to the lower surface of the slabs.
- The instantaneous difference between the total pressure acting on the upper surface, p, and the pressures acting on the lower surface of the slab, p_u, can reach high values, occasionally causing the total uplift force to exceed the weight of the slab.
- The instantaneous spatial structure of the pressure fluctuations may play a relevant role in the magnitude of the overall lifting force.

Traditionally, scale physical hydraulic models are used to evaluate the uplift force generated by the pressure fluctuations in hydraulic structures. However, this approach can be prohibitively expensive in terms of time and cost, and the internal flow field of the hydraulic jump cannot be investigated. The use of the CFD simulations could become a solution to overcome these issues.

The aim of the paper is to evaluate the uplift forces acting on the slabs under the hydraulic jumps using results from physical hydraulic model and CFD modelling. The results of CFD are compared and validated against the outcomes of physical hydraulic model tests. Furthermore, the design of the slabs using sealed and unsealed joints are compared and some important considerations are noted.

Methodology

With reference to Figure 1, Fiorotto and Rinaldo (1992a) proposed a design criterion based on geometric parameters and the magnitude of the uplift force induced by severe fluctuations associated with energy dissipation in the hydraulic jump zone, giving the stable slab thickness, s, in the case of unsealed joints as:

$$s = \Omega\left(\frac{L_x}{y_1}, \frac{L_x}{I_x}, \frac{L_y}{I_y}\right)\left(c_p^+ + c_p^-\right)\frac{u_1^2}{2g}\frac{\gamma}{\gamma_c - \gamma} \quad (1)$$

where Ω = dimensionless coefficient related to the instantaneous spatial distribution of the pulsating pressures for unsealed joints; y_1 = depth of incident flow; L_x and L_y = slab length and width; I_x and I_y = turbulence integral scales along the flow direction and transversally; c_p^+ and c_p^- = coefficients of positive and negative pressure fluctuations; $u_1^2/2g$ = kinetic energy head of the entering flow where u_1 is the mean velocity of inlet flow and γ and γ_c = specific weights of water and concrete. The use of Eq. (1) for design requires the evaluation of the maximum positive and negative fluctuating pressures, as well as the evaluation of the reduction factor, Ω, for unsealed joints, as follows:

$$\Omega = \frac{1}{2\sigma_p N_s}\Big(\Sigma_k \Sigma_{i=1}^{N_s}\Sigma_{j=1}^{N_s}\hat{p}_{k,i}\hat{p}_{-k,j} + \Sigma_k \Sigma_{i=1}^{N_s}\Sigma_{j=1}^{N_s}\Sigma_{k1=1}^{N_b}\Sigma_{k2=1}^{N_b}\alpha^*_{k,k1,i}\alpha^*_{-k,k2,j}\hat{p}_{k,k1}\hat{p}_{k,k2} -$$

$$2\Sigma_k \Sigma_{i=1}^{N_s}\Sigma_{j=1}^{N_s}\Sigma_{k3=1}^{N_b}\alpha^*_{k,k3,j}\hat{p}_{k,k3}\hat{p}_{-k,i}\Big)^{1/2} \quad (2)$$

Where $\hat{p}_k$ = spectral components of the fluctuating pressures, σ_p = standard deviation of the fluctuating pressures, N_s is the number of sub-areas the slab is divided into, *i*, *j* = position indexes of the slab sub-area; *k*1, *k*2, *k*3 = position indexes at the N_b points along the unsealed joints; $\alpha^*_{k,k1,i}$ = ratio between the underside pressure in *i* and the pressure at the *k*1 edge, for the wave number *k*.

This last parameter, $\alpha^*_{k,k1,i}$, is obtained by computing the pressure value at the *i* position under the slab, produced by a pressure $\hat{p}_k = 1$ at the *k*1 edge and $\hat{p}_k = 0$ at the other edges via the pressure propagation equation within the foundation layer (Fiorotto and Caroni 2014).

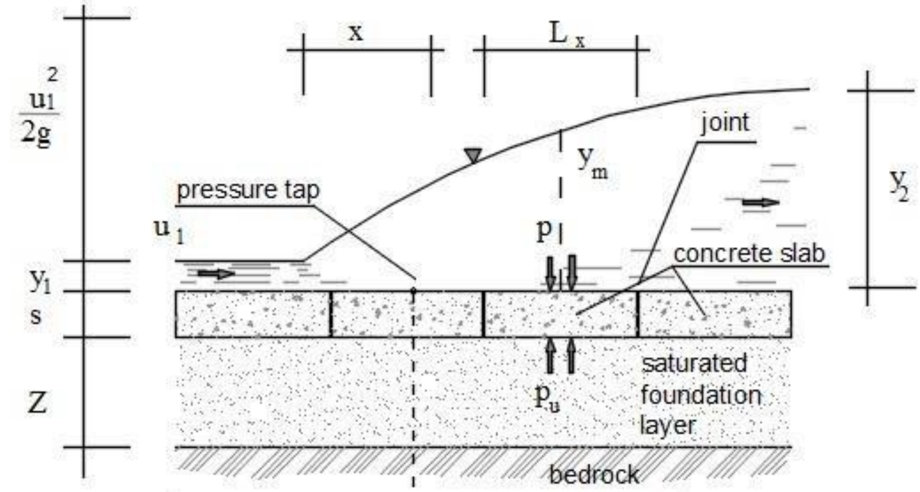

***Figure 1**: Slab stability scheme – (Barjastehmaleki et al. 2016a)*

The three terms on the right side of Eq. (2) account for the following:

- The first term – the pressures acting on the slab
- The second term – the pressures underneath the slab transferred through the unsealed joints
- The third term – the simultaneous pressures acting at the upper and lower slab surfaces, being transferred through the unsealed joints

The dimension of the stable stilling basin slabs can be computed using Eq. (1) for the case of slabs with sealed joints. The Ω value can be obtained using the results presented by Barjastehmaleki (2016b) and values of c_p^+ and c_p^- can be evaluated according to data in Toso and Bowers (1998) and Fiorotto and Rinaldo (1992). The application of results presented in the literature, related to the c_p and Ω coefficients, can lead to overestimation in the equivalent slab thickness, mainly due to the challenge in extrapolating to practical cases, where the overall geometry may differ significantly from the cases examined in the literature. This is evidenced in the 'Design example' section of this paper.

A method for a more accurate evaluation of the slab thickness is presented here by direct evaluation of uplift force, F'_{max}, using the results of physical hydraulic modelling and CFD. In physical hydraulic model, the uplift force is measured using force transducers. In CFD, the pressure over the slab is obtained, but the pressure field under the slab is calculated via numerical solution of Laplace equation imposing the instantaneous values of pressures along the slab boundary as the boundary condition. The finite difference numerical scheme is given in Eq. (3).

$$\frac{\partial^2 P}{\partial x^2} + \frac{\partial^2 P}{\partial y^2} = \frac{P_{i+1,j} - 2P_{i,j} + P_{i-1,j}}{\Delta x^2} + \frac{P_{i,j+1} - 2P_{i,j} + P_{i,j-1}}{\Delta y^2} \quad (3)$$

where the two subscripts in P define the computing points index, one for i or x direction and the other for j or y direction (as defined in Figure 2), and Δx and Δy are the distance between these points in the x and y directions. This scheme is second order accurate.

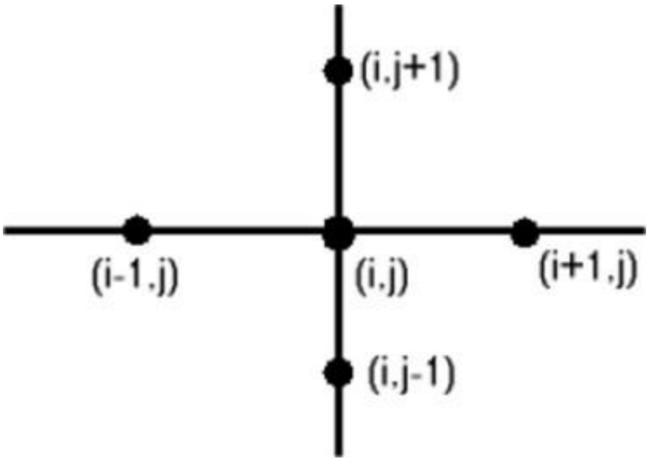

Figure 2: Five points Laplace Equation finite difference numerical scheme

Assuming $\Delta x = \Delta y$, according to Eq. (3), the following system is obtained:

$$P_{i+1,j} - 2P_{i,j} + P_{i-1,j} + P_{i,j+1} - 2p_{i,j} + P_{i,j-1} = 0 \quad (4)$$

This equation is written for all the points inside the slab computational domain, while along the domain boundary where points with index [i+1, j], [i-1,j], [i,j+1] and [i,j-1] happen, the pressure P is imposed equal to the one computed in these points by CFD.

The bottom turbulent pressure fluctuating field is obtained in the CFD analysis at a discrete number of points according to the computational mesh size. The distance between two points in x and y directions, on the bottom channel, are Δx and Δy, respectively. If N is the total number of CFD computation points in the slab area and P_i the instantaneous value of the pressure computed in the i^{th} point, the instantaneous force, F_s, acting on the upper face of the slab area is:

$$F_s = \Sigma_{i=1}^{N}(P_i \Delta x \Delta y) \quad (5)$$

The instantaneous uplift force, F_u, results from the propagation, through the joints and the substrate, of the fluctuating pressure which acts along the slab joints. This is obtained at the CFD computation points along the slab boundary in the CFD computational domain. These instantaneous pressures are propagated under the slab according to Laplace equation. The numerical solution of the Laplace equation using finite difference yields the uplift pressure, $P_{u,i}$, at every numerical computation point with subscript, i. The imposed boundary conditions are the instantaneous pressures computed along the slab boundary in the CFD modelling. The distance between two points in the x and y direction, under the slab are Δx and Δy, respectively. If N is the total number of Laplace equation computational grid points under the slab area, the instantaneous value of the uplift force on the base of the slab is:

$$F_u = \Sigma_{i=1}^{N}(P_{ui} \Delta x \Delta y) \quad (6)$$

The total force, F, acting instantaneously on the slab is:

$$F = F_u - F_s \quad (7)$$

Physical model experimental setup and procedure

A large gravity dam was modelled at a 1:40 geometric scale, according to the Froude similarity. The height of the dam at the spillway was 47.35 m with a downstream face slope of 0.8H:1V. The stilling basin was 46.75 m long, 80 m wide. With reference to the previous studies on the Ω coefficient, and technical and economical constraints, a rectangular slab with prototype length l_x = 8 m (upstream-downstream) and width l_y = 4 m (cross valley) was chosen. At the downstream end of the stilling basin, a weir 3.3 m high was provided to control the position of the hydraulic jump.

The experimental setup is shown in Figure 3 and Figure 4. An aluminium frame, 1000 mm long, 500 mm wide and 25 mm thick, was inserted in the stilling basin invert. Inside the hollow, five movable aluminium slabs each 200 mm long (8 m prototype), 100 mm wide (4 m prototype) and 8 mm thick was cast with the upper face at the same level (up to O(10^{-5}) m accuracy) as the invert of the stilling basin .

The dimensions of the hollow were such as to leave a gap of about 2 mm along the slabs sides. Through this gap, the fluctuating pressures at the bottom of the hydraulic jump propagate in a 2 mm thick water layer under each slab. This pressure propagation takes place with negligible friction resulting in minimal reduction of the transmitted uplift pressures. This is in accordance with the theoretical analysis as applied to real cases presented in Fiorotto & Rinaldo (1992a). By neglecting damping as a result of friction, a safer result is obtained.

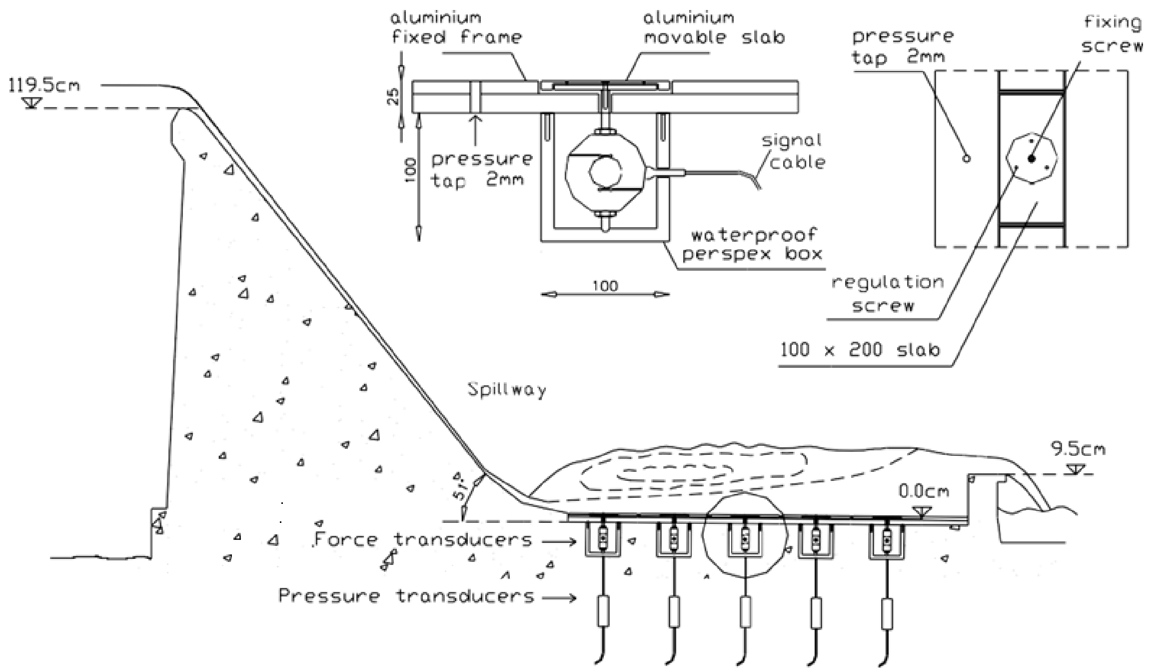

Figure 3: Experimental setup of a stilling basin downstream of a large dam

Figure 4: View of the experimental installation (left) and the test frame within the stilling basin (right)

The alignment of the upper face of the movable slabs with the basin bottom is a crucial problem to address in the modelling as even a minor misalignment can affect the pressure field around the slab, thus inducing errors in the measured forces. For this reason, the movable slabs were fixed by means of three micrometric regulation screws and a fixing screw, to a circular plate coupled to the force transducers (Figure 3).

Both the movable slabs and the circular coupling plate and the joint (hollowed) were built in aluminium, to be as light as possible, whilst maintaining the requirements of resistance and stiffness, to minimise the inertial effect on force measurement.

Each force transducer was placed in a rigid waterproof Perspex box, with 10 mm thick walls. This box was fixed to the aluminium frame. The joint connecting the movable slabs to the force transducers have a smaller diameter than the hole in the frame to avoid friction effects on force measurement. As a consequence the water in the Perspex box is directly connected with the water film under the movable slabs. Thus a rigid waterproof container is needed, to prevent any damping of the pressure propagation and vibration of the force transducers which are fixed to the base of the perspex box.

Force transducers (Model No TS100 provided by AEP Transducers) with a sensitivity less than 0.1 N, and a response time less than the microscale time of the pulsating forces were used. The choice of this type of force transducer was conditioned by the need to cope with measurement accuracy, hardware robustness compatible with use in large hydraulic models, waterproof sealing (IP68) to operate in submerged conditions, and long duration dynamic applications. The signal was amplified and conditioned via TA4 analog transmitters (AEP Transducers), with a frequency response of 1 kHz.

Five pressure tappings were inserted on the stilling basin invert, aligned with the centre of each slab at a distance from the toe of the spillway as summarised in Table 1. The pressure tappings had a diameter of 2 mm and were connected to the pressure transducers by a rigid tube of 4 mm internal diameter. Pressure transducers of type Foxboro FPT adjusted in the range 0-70 kPa, with a response time less than 1 ms, that is, lower than the microscale time of the pulsating pressure (Abdul Kader & Elango 1974), were adopted.

Table 1: Layout of model pressure tappings

Tapping	No 1	No 2	No 3	No 4	No 5
Model distance from spillway toe (m)	0.1	0.3	0.5	0.7	0.9
Prototype distance from spillway toe (m)	4	12	20	28	36

The following instrumentation setup was used in the PHM:

- The transducers were linked to a computer using a 64 channel analog-digital board (United Electronic Instruments PD2-MF- 64-400/14H).
- Sampling was performed by means of the Dasylite code by Dasytech USA.
- The inflow discharge was measured by an induction flow meter (MUT 2200 316 L by Automazioni Industriali, Padua, Italy) with an instrumental accuracy lesser than 0.2% and significant digits of 0.1 L/s.

Computational Fluid Dynamics (CFD) modelling

CFD models of the physical model experimental setup were developed for comparison against the equivalent physical scenario to investigate whether numerical techniques can yield a valid dataset for analysis of the pressure fluctuations related to concrete slabs in stilling basins.

All modelling was undertaken using Siemens Star CCM+, which is a CFD modelling package that is widely used by commercial and research organisations.

The CFD models featured an equivalent geometry setup to the scale physical hydraulic model. The time of the simulations was equal to 20 minutes and a sampling rate of 100 Hz was adopted to provide results comparable to the experiment.

The following boundary conditions were applied in the CFD models:

- The inlet to the model was configured as a flow boundary condition in which a fixed discharge value is distributed over a cross sectional flow area
- The outlet of the model was configured as a zero pressure boundary to allow the free exit of flow from the model domain
- A no-slip shear wall condition was applied on the model base and walls to simulate the effects of wall roughness applicable to concrete
- A symmetry condition was applied at the top of the model.

The CFD simulations featured the following key physics models:

- Multi-phase flow (air and water)
- Isothermal flow conditions
- Constant density and dynamic viscosity
- Volume of Fluid (VOF) approach
- Gravity (9.81 m/s^2 in the negative Z axis)
- Implicit unsteady solver with an applied time-step of 0.01s;
- Detached Eddy Simulation (DES) turbulence model.

The volume mesh that was generated for the modelling task featured a variable cell size ranging from 2 mm to 100 mm and comprised approximately 15 million cells. Prism meshing (inflation of the mesh along wall boundaries) and targeted cell size refinement was utilised throughout the CFD model domain to ensure sufficiently fine mesh at all solid boundaries and key regions of interest. As a part of the CFD modelling, different mesh resolutions were tested to optimise performance in relation to precision and computational time. The error in outputs using smaller mesh size resulted less than 3%.

The simulation was run using a K-ω based DES turbulence model. It is well understood in hydrodynamics that the current industry approach to CFD modelling using k-ε turbulence models is typically insensitive to adverse pressure gradients (Ansys Fluent 12.0). As a result, k-ε turbulence models are not able to correctly reproduce the detailed turbulent eddies and associated local pressure fluctuations at the water-solid interface as is the case when considering stability of slabs in stilling basins and plunge pools. Such models can result in overly optimistic design evaluations for flows that separate from smooth surfaces.

DES is a modification of a RANS model in which the model switches to a sub-grid scale formulation in regions fine enough for LES calculations. Regions near solid boundaries and also where the turbulent length scale is less than the maximum grid dimension are assigned the RANS mode of solution. As the turbulent length scale exceeds the grid dimension, the regions are solved using the LES mode – in this way the grid size can be chosen with reference to the scale of turbulence relevant to the problem. This method of simulating turbulence has the potential to correctly reproduce the detailed turbulent eddies and associated local pressure fluctuations in the regions of interest, while remaining less computationally intensive than undertaking a full LES model. Pressure fluctuations at the boundary of the slabs are recorded in a grid with 1 cm spacing, and also at five points representing the location of the PHM pressure taps as listed in Table 1.

Results and Discussion

All the CFD and physical hydraulic model tests were undertaken at a 1:40 geometric scale, while the scales for other parameters (Table 2) can be obtained on the assumption that the motion, influenced mainly by gravitational and inertial forces, has the same Froude number in the prototype and in the model.

Table 2: Summary of PHM scales

Parameter	Scale
Distances and heights	1:40
Velocity	1:6.32
Time	1:6.32
Discharges	1:10,119
Pressures	1:40
Force on slabs	1:64,000

The design discharge of 800 m^3/s was tested in the physical hydraulic and CFD models. Images of the models operating are included in Figure 5. The flow characteristics in the stilling basin are summarised in Table 3. The estimation of the flow characteristics in the zone of hydraulic jump using PHM is a difficult task. However, using CFD, an accurate evaluation of the flow characteristics was achievable.

Table 3: Stilling basin flow characteristics

Parameter	PHM		CFD	
	Model	Prototype	Model	Prototype
Discharge (m^3/s)	0.08	800	0.08	800
Initial velocity (m/s)	3.84	24.30	3.80	24.00
Initial depth (m)	0.01	0.41	0.01	0.42
Froude number	12.00	12.00	12.00	12.00
Run duration (min)	20	126	20	126

Figure 5: Physical model in operation

The pressure data obtained from CFD and the PHM were analysed to evaluate the thickness of a stable slab using Eq. (1),. Pressure time series $p(t)$ are a random stationary process (Vasiliev and Bukreyev 1967), thus, it is convenient to use the pressure fluctuations, $p'^{(t)} = p(t) - \bar{p}$, around the mean pressure value, $\bar{p}$. The are The maximum measured positive and negative pressure fluctuation values are p'^{+}_{max} and p'^{-}_{max}, respectively. The fluctuations under the jump are usually related to the kinetic energy of the jet entering the stilling basin, $u_1^2/2g$, by means of the pressure coefficients, c_p^+ and c_p^-, (Toso & Bowers, 1988, Fiorotto & Rinaldo 1992b) as follows:

$$c_p^+ = \frac{P'^{+}_{max}}{\gamma \frac{u_1^2}{2g}} \quad (8)$$

$$c_p^- = \frac{P'^{-}_{max}}{\gamma \frac{u_1^2}{2g}} \quad (9)$$

The values of Ω and the pressure coefficients, c_p^+ and c_p^-, required for Eq. (1) are presented in Table 4. In order to avoid the need to estimate values of c_p and Ω, the uplift force was directly evaluated. This was done by direct force measurement in the physical hydraulic model, and using Eq. (5) to (9) from the CFD results.

A comparison of the results from the PHM and CFD analyses is presented in Table 4. From this, the following points are noted:

- The results obtained using the CFD approach is in good agreement with PHM results.
- With reference to the pressure fluctuations, the c_p values are of the same order of magnitude of those ones computed by Fiorotto & Rinaldo (1992b) and Toso & Bowers (1988), taking into account the different characteristics of the inflow conditions and of the hydraulic jump position. In fact, the peak values of c_p at the beginning of the stilling basin, since the toe of the hydraulic jump is located on the spillway chute, upstream of the stilling basin (Fig. 5); and
- The maximum value of the Ω coefficient ranges between 0.10-0.15. This value is close to the value 0.15, which can be obtained from the experimental results given in Barjastehmaleki et al. (2016b).
- The force, F^+, acts in a downward direction and F^- acts in an upward direction.

Table 4: Summary of PHM and CFD results

Parameter	PHM results by slab number					CFD results by slab number				
	1	2	3	4	5	1	2	3	4	5
c_p^+	0.41	0.26	0.23	0.15	0.1	0.47	0.25	0.23	0.14	0.1
c_p^-	0.33	0.28	0.25	0.19	0.12	0.32	0.26	0.25	0.2	0.1
F^+_{max} (N)	13.1	8.1	6.30	4.10	0.6	13.3	9.0	6.2	4.3	0.6
F^-_{max} (N)	-12.3	-1.1	-0.8	-0.5	-0.04	-13.0	-1.5	-1.0	-0.6	-0.05
Ω	0.13	0.12	0.1	0.08	0.02	0.13	0.1	0.1	0.08	0.02

Design example

From the graphs in Barjastehmaleki et al. (2016b), for l_y/y_1= 9.6 and l_x/y_1= 19.2, one can obtain Ω = 0.15. Assuming a value of c_p^+ and c_p^- equal to 0.7 according to data by Toso & Bowers (1988), and using Eq. (1), an equivalent thickness of the slab equal to 3.6 m is obtained. Obviously, this value is a conservative estimation (due to conservative values of c_p^+ and c_p^-), and for important structures, a more accurate evaluation can be obtained by use of PHM or CFD.

The experimental results presented in Table 4 allow calculation of the equivalent slab thickness required to ensure the stability of the lining in the spillway stilling basin

From the PHM, the equivalent slab thickness can be computed directly using the measured forces with Eq (10) or using the pressure measurements with Eq. (1). Using the CFD modelling results, the equivalent slab thickness is calculated using Eq (1).

$$s = \frac{max(F_{max}^{+}, F_{max}^{-})}{l_x l_y (\gamma_c - \gamma)} \quad (10)$$

Computation of the equivalent thickness is presented in Table 5, assuming a specific weight for concrete and water equal to 25 kN/m³ and 10 kN/m³, respectively. It should be noted that an appropriate factor of safety must be applied to these results to account for model simplifications, scale effects and the sampling duration etc.

Table 5: Computation of the equivalent slab thickness

Parameter	From PHM results by slab number					From CFD results by slab number				
	1	**2**	**3**	**4**	**5**	**1**	**2**	**3**	**4**	**5**
F'_{max} (kN)	838	518	403	262	38	851	576	397	275	38
s (m)	1.7	1.0	0.8	0.5	0.1	1.9	1.2	0.8	0.6	0.1

With reference to the calculation above which yielded a thickness of 3.6 m, this alternative approach has yielded a reduction in slab thickness of approximately 50%.

Conclusion

The paper presents the results of a study on the pressure fluctuations under hydraulic jumps in stilling basins based on physical hydraulic and CFD modelling. The results presented in Table 5 show that the proposed DES CFD approach together with the Laplace formulation for propagation of the pressure under the slab is capable of evaluating the required slab thickness in the case studied here. This approach was validated against direct force measurements from a physical hydraulic model. It is also shown that the use of the values for the coefficients of the maximum pressure fluctuations (c_p^+ and c_p^-) reported in the literature may yield an overestimation of the slab thickness. When considering this as it applies to large dams, this example gives an indication of the potential project benefits in terms of optimisation of the stilling basin slab design which can be achieved through CFD or experimental assessment of the fluctuating pressures in the hydraulic jump.

References

Abdul Khader, M. H., and Elango, K. (1974). “Turbulent pressure field beneath a hydraulic jump.” J. Hydraul. Res., 12(4), 469–489.

ANSYS Fluent 14.0 [Computer software]. ANSYS, Canonsburg, PA.

Barjastehmaleki, S., Fiorotto, V., and Caroni, E. (2016a). "Spillway Stilling Basins Lining Design via Taylor Hypothesis." *J. Hydraul. Eng.*, 10.1061/(ASCE)HY.1943-7900.0001133, 04016010.

Barjastehmaleki, S., Fiorotto, V., and Caroni, E. (2016b). "Design of Stilling Basin Linings with Sealed and Unsealed Joints." *J. Hydraul. Eng.*, 10.1061/(ASCE)HY.1943-7900.0001218, 04016064.

Bellin, A., and Fiorotto, V. (1995). “Direct dynamic force measurement on slab in spillway stilling basin.” J. Hydraul. Eng., 10.1061/(ASCE)0733- 9429(1995)121:10(686), 686–693.

Bowers, C. E., and Toso, J. (1988). “Karnafouli project, model studies of spillway damage.” J. Hydraul. Eng., 10.1061/(ASCE)0733-9429(1988) 114:5(469), 469–483.

Bowers, C. E., and Tsai, F. H. (1969). “Fluctuating pressure in spillway stilling basins.” J. Hydraul. Div., 95(6), 2071–2080.

Chow, V. T. (1959). “Open-channel hydraulics.” New York: Mc Graw Hill.

Fiorotto, V. and Caroni, E. (2014). "Unsteady Seepage Applied to Lining Design in Stilling Basins." *J. Hydraul. Eng.*,

10.1061/(ASCE)HY .1943-7900.0000867, 04014025.

Fiorotto, V., and Rinaldo, A. (1992a). “Fluctuating uplift and lining design in spillway stilling basins.” J. Hydraul. Eng., 10.1061/(ASCE)0733- 9429(1992)118:4(578), 578–596.

Fiorotto, V., and Rinaldo, A. (1992b). “Turbulent pressure fluctuations under hydraulic jump.” J. Hydraul. Res., 30(4), 499–520.

Fiorotto, V., and Salandin, P. (2000). “Design of anchored slabs in spillway stilling basins.” J. Hydraul. Eng., 10.1061/(ASCE)0733-9429(2000) 126:7(502), 502–512.

Sanchez Bribiesca, J. S., and Capella Viscaino, A. C. (1973). “Turbulent effects on the lining of stilling basin.” Proc., 11th Int. Congress on Large Dams, Vol. 11, Madrid, Spain, 1575–1592. Toso, J. W., and Bowers, C. E. (1988). “Extreme pressures in hydraulic jump stilling basins.” J. Hydraul. Eng., 10.1061/(ASCE)0733-9429 (1988)114:8(829), 829–84.

Vasiliev, O. F., and Bukreyev, V. I. (1967). “Statistical characteristics of pressures fluctuations in the region of hydraulic jump.” Proc., 12th Congress, Int. Association of Hydraulic Research, Vol. 2, Fort Collins, CO.

USBR “Design of small dams.” (1977). Washington, D.C.: Water Resources Tech. Publications.